Chinese Chemical Letters 32 (2021) 3155–3158

Contents lists available at ScienceDirect

Chinese Chemical Letters

journal homepage: www.elsevier.com/locate/cclet

Communication

Target-induced mimic enzyme deactivation based on mixed-node metal-organic frameworks for colorimetric assay of hydrogen sulfide

Fenfen Zhou[a], Yanli Zhou[b,*], Jianwei Zhang[b], Hui Dong[a,b], Lantao Liu[a,b], Yintang Zhang[b], Maotian Xu[a,b]

[a] College of Chemistry, Zhengzhou University, Zhengzhou 450001, China
[b] Henan Key Laboratory of Biomolecular Recognition and Sensing, College of Chemistry and Chemical Engineering, Shangqiu Normal University, Shangqiu 476000, China

ARTICLE INFO

Article history:
Received 8 December 2020
Received in revised form 18 January 2021
Accepted 23 February 2021
Available online 26 February 2021

Keywords:
Metal-organic frameworks
Hydrogen sulfide
Colorimetric assay
Deactivation
Mimic enzyme

ABSTRACT

Accurate detection of hydrogen sulfide (H_2S) is of great significance for environmental monitoring and protection. We propose a colorimetric method for the detection of H_2S by the use of mixed-node Cu-Fe metal organic frameworks (Cu-Fe MOFs) as highly efficient mimic enzymes for target-induced deactivation. The Cu-Fe MOFs were synthesized by a simple solvothermal method and could catalyze the H_2O_2 mediated oxidation of 3,3′,5,5′-tetramethylbenzidine (TMB) to oxTMB with a blue color. The presence of dissolved H_2S would deactivate the mimic enzymes, and then the blue color disappeared. The mechanism of the sensor was discussed by steady-state kinetic analysis. The designed assay was highly sensitive for H_2S detection with a linear range of 0–80 μmol/L and a detection limit of 1.6 μmol/L. Moreover, some potential substances in the water samples had no interference. This method with the advantages of low cost, high sensitivity, selectivity, and visual readout with the naked eye was successfully applied to the determination of H_2S in industrial wastewater samples.

Metal-organic frameworks (MOFs) as a class of highly porous crystalline materials play as crucial role in sensing of target analytes due to their superior frameworks and structural attributes, such as extremely high surface area, and large functional sites and porosity [1,2]. For the MOF materials, plenty of coordination nodes and organic linkers can produce essentially infinite number of possible combinations. Their pore sizes are from several angstroms to several nanometers and their structures for different target molecules could be tuned by the selection of metal ions and organic linkers. Thus, beyond the accessible porosity, the versatile functionalities including catalysis, electricity, fluorescence, and luminescence make them an excellent platform for highly selective and sensitive detection of various analytes [3–7].

The monitoring and control of dissolved hydrogen sulfide (H_2S) in natural and waster waters have been in demand for a long time because its level is an important environmental index [8,9]. With the aim of real-time, miniaturized, and highly selective detection of H_2S, nanomaterials (*e.g.*, carbon-based nanomaterials, metal nanoparticles, metal oxide nanoparticles, and quantum dots) have been utilized [10–15]. In recent years, the MOF-based detection of H_2S have been widely researched in terms of fluorescent, cataluminescent, and electrochemical properties [16]. The MOF-based sensors mainly rely on host-guest interactions between the metal ions of MOFs and S^{2-}. For the fluorescent and cataluminescent detection of H_2S [17–30], pre- and post-synthetic modification methods of MOFs like incorporating functional groups of azide, nitro, or vinyl have been illustrated as effective strategy to improve the sensing performance. However, the critical challenges associated with this technique were the maintenance of long-term photostability and the complex synthesis routes of MOFs. On the account of the electrocatalytic activity of MOFs, the MOF composites were modified on the electrode surfaces for the electrochemical sensing of H_2S [31,32]. Interestingly, the synergistic combination of MOFs and active components could provide the outstanding characteristics. The MOFs as excellent host matrics were not only served as nanocarriers for electroactive materials but also worked as catalysts for H_2S oxidation. Nevertheless, the low signal transduction capacity was still a problem for its high sensitive detection. Hence, it is desirable to explore an efficient MOF-based method for sensitive and selective analysis of H_2S.

Very recently, MOF-based colorimetric assays have been reported based on the catalytic activity of the mimic enzymes

* Corresponding author.
E-mail address: zhouyanli@mails.ucas.ac.cn (Y. Zhou).

https://doi.org/10.1016/j.cclet.2021.02.053
1001-8417/

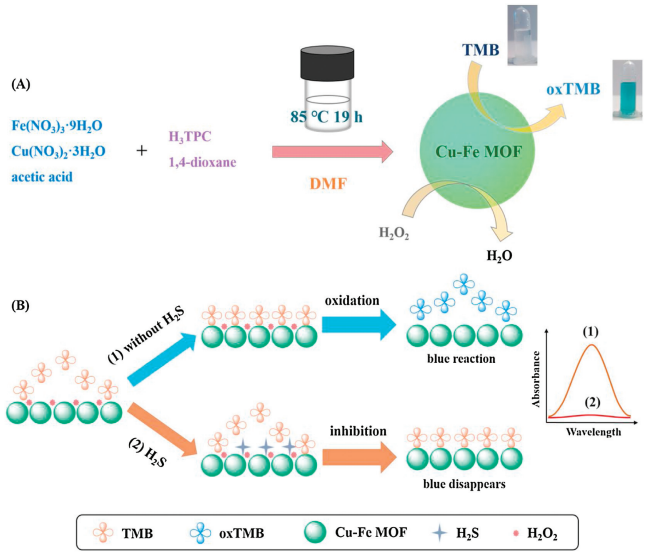

Scheme 1. (A) Synthesis of Cu-Fe MOFs and color change after reaction with TMB. (B) Colorimetric detection of H_2S by using Cu-Fe MOFs as peroxidase mimics.

[33]. They have demonstrated obvious advantages over natural enzymes in terms of good stability, high efficiency, low cost, and easy storage. Furthermore, the unique physicochemical characteristics of MOFs endow MOF-based mimic enzymes with multiple functionalities *via* the rational design. The studies on colorimetric sensing have manifested MOFs as useful peroxidase mimics for the detection of hydrogen peroxide (H_2O_2), glucose, and some reducing agents like ascorbic acid [34–37]. By contrast, the potential of MOFs as mimic enzymes has rarely been exploited for the evaluation of levels of H_2S [38,39]. The unsatisfactory catalytic activity of single component MOFs might limit their application in colorimetric sensors.

In this contribution, we presented a mixed-node Cu-Fe MOF as the mimic enzyme for the colorimetric detection of H_2S based on the target-induced deactivation effect. In Scheme 1A, the mixed and high-density open metal sites of Cu-Fe MOFs were synthesized by a simple one-pot approach under the control of reacting temperature and reactant ratio [40]. The mixed Cu-Fe MOFs were constructed from a well-known paddle-wheel-like $[Cu_2(COO)_4]$ dimer and a $[Fe_3(\mu_3\text{-}O)(COO)_6]$ trimeric cluster. The morphology and structure of Cu-Fe MOFs were identified by scanning electron microscope (SEM) and X-ray diffraction (XRD). In Fig. 1a, Cu-Fe MOFs formed petal ellipsoid aggregates which was composed of cross-linked sheets with 5–10 micrometers (μm) in size. The XRD patterns of Cu-Fe MOFs (Fig. 1b) showed that the as-obtained samples were crystalline and its diffraction peaks were consistent with the simulated samples which previously reported [40]. The elemental mapping in Figs. 1c–f demonstrated the even distribution of Cu and Fe element, which signified the location of both Cu and Fe species in the crystal lattices of Cu-Fe MOFs. The energy dispersive spectrometer (EDS) analysis (Fig. S1 in Supporting information) revealed that the atomic ratio of Cu/Fe in the Cu-Fe MOFs was 2/1.

The peroxidase-like activity of Cu-Fe MOFs was evaluated by the catalytic oxidation of 3,3′,5,5′-tetramethylbenzidine (TMB) in the presence of H_2O_2. Typical absorption spectra of TMB in different reaction systems were illustrated in Fig. 2a. The solution of TMB in NaAc-HAc buffer just had a background absorption, and its color was colorless. When only H_2O_2 was added, the absorption curve was nearly unchanged and the solution color was light blue (near colorless) due to the partial oxidation of TMB. Meanwhile, when just MOF was added, the background absorption of Cu-Fe

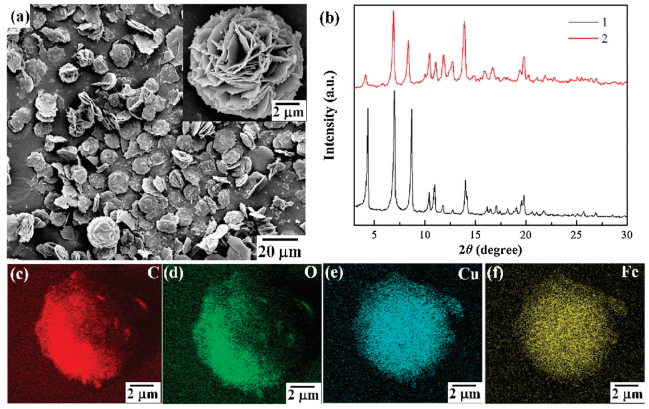

Fig. 1. Low-magnification SEM image (a), high-magnification SEM image (inset of a) of Cu-Fe MOFs. (b) XRD pattern of Cu-Fe MOFs before (1) and after (2) binding with H_2S. Elemental mapping of Cu-Fe MOFs: C (c), O (d), Cu (e) and Fe (f).

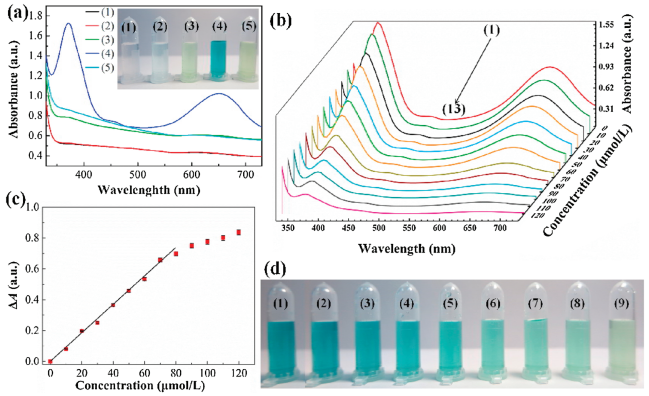

Fig. 2. (a) Typical absorption spectra and photographic image (inset) of TMB (1), TMB + H_2O_2 (2), TMB + MOF (3), TMB + H_2O_2 + MOF (4) and TMB + H_2O_2 + MOF + H_2S (5). UV–vis spectra (b), trend chart of absorption peak and concentration dependence (c), and photographic image (d) of the colorimetric assay with the increasing concentrations of H_2S: (1) 0, (2) 10, (3) 20, (4) 30, (5) 40, (6) 50, (7) 60, (8) 70, (9) 80, (10) 90, (11) 100, (12) 110 and (13) 120 μmol/L. Conditions: TMB, 1.4 mmol/L; H_2O_2, 0.56 mmol/L; Cu-Fe MOFs, 0.30 mg/mL; the buffer solution was 0.1 mol/L NaAc-HAc solution (pH 3.5).

MOFs was observed and the solution appeared light green color of Cu-Fe MOFs, indicating that TMB did not react with Cu-Fe MOFs directly. On this basis, the Cu-Fe MOFs catalyzed the oxidation of TMB to oxTMB with a blue color in the presence of H_2O_2, and there was a strong absorbance peak at 652 nm. Obviously, the Cu-Fe MOFs behaved like peroxidase toward typical TMB substrate. Interestingly, after the induction of H_2S into this system, the absorption peak disappeared rapidly and the color was expected to change from blue to light green. The addition of H_2S caused the deactivation of the peroxidase mimic, which might be ascribed to the occupation by H_2S on the active sites of Cu-Fe MOFs. Thus, oxidation-induced blue color generation could be efficiently inhibited by H_2S. In addition, after the above catalytic oxidation and combination, the XRD data (Fig. 1b) still remained the same patterns with the Cu-Fe MOFs, proving the high stability of the Cu-Fe MOFs. In view of this, a simple colorimetric method for H_2S detection was proposed in Scheme 1B.

Similar to horseradish peroxidase (HRP) enzyme, the catalytic activity of Cu-Fe MOFs as enzyme mimics is also dependent on pH and substrate concentration. Therefore, to obtain the best sensing performance of Cu-Fe MOFs for H_2S detection, key parameters including buffer pH, quantity of Cu-Fe MOFs, concentration of H_2O_2 or TMB were systematically varied and optimized in this study. The

absorption difference (ΔA) after and before the addition of H_2S was utilized as the parameter of colorimetric assay. Firstly, catalytic activity of Cu-Fe MOFs in a series of NaAc-HAc buffer solution with different pH values was evaluated from pH 3–6 in Fig. S2a (Supporting information). It was found that there was strong absorption response in the acidic solution, which might be due to the fact that acidic solution could provide more H^+ and promote the catalytic oxidation of TMB in the presence of H_2O_2 [41,42]. Thus, 0.1 mol/L NaAc-HAc buffer solution (pH 3.5) was selected as the optimal reaction medium. The Cu-Fe MOFs were further controlled to find out the suitable quantity for effective response to H_2S (Fig. S2b in Supporting information). As the quantity of Cu-Fe MOFs was less than 0.30 mg/mL, the performance of the colorimetric assay gradually increased. The response reached a maximum value when its quantity was 0.30 mg/mL and then decreased. Therefore, 0.30 mg/mL of Cu-Fe MOFs was fixed as the optimal quantity for the following studies. By analogy, other optimum conditions were obtained: 1.4 mmol/L TMB and 0.56 mmol/L H_2O_2 (Figs. S2c and S2d in Supporting information). These results were close to the values obtained with other mimics and HRP [41,42].

To further analyze the catalytic mechanism, a comparison of detection of H_2S using the colorimetric system was investigated by use of the Cu-Fe MOFs and monometallic Cu-MOFs and Fe-MOFs (Fig. S3 in Supporting information). For the Cu-MOFs, low catalytic activity for the oxidation of TMB was observed. After the addition of H_2S, the absorption peak could decrease rapidly and the solution changed to nearly colorless, indicating that the Cu-MOFs had strong binding with H_2S. Clearly, the Fe-MOFs showed high catalytic activity for the oxidation of TMB, whereas the absorption peak and the solution color had unnoticeable changes for detection of H_2S. Compared with the monometallic Cu-MOFs and Fe-MOFs, the biggest ΔA and the obvious color change by the use of Cu-Fe MOFs could be obtained for detection of H_2S, which was attributed to the combined properties of strong binding ability from Cu and catalytic activity from Fe. The catalytic activity of Cu-Fe MOFs was also studied by enzyme kinetics theory with H_2O_2 and TMB as substrates. The steady-state kinetic parameters including Michaelis-Menten constant (K_m) and maximum initial velocity (V_{max}) were investigated by changing the concentrations of TMB or H_2O_2 in this system while other variables remained unchanged. Three typical Michaelis-Menten curves was obtained (Figs. S4a, S4c, S5a and S5c in Supporting information) in a certain range of substrate concentration. The results demonstrated that the oxidation reaction catalyzed by Cu-Fe MOFs and HRP agreed with the typical Michaelis-Menten behavior towards substrate TMB. The K_m and V_{max} were obtained by showing the slope and intercept of the double reciprocal line graph from Michaelis-Menten equation [25,37]. Smaller K_m values indicate stronger affinity between the enzyme and the substrate. In Table S1 (Supporting information), the apparent K_m of MOF with H_2O_2 and TMB as substrate was much lower than that of HRP, which suggested that MOF had relatively high affinity for substrate than HRP. This could be attributed to the combined catalytic activity from bimetallic Cu-Fe MOFs. The double-reciprocal plots V_0 and [S] revealed that a series of lines intersected at the negative half axis of the reciprocal of concentration (Figs. S4b, S4d, S5b and S5d in Supporting information). The K_m value remained constant, but V_{max} value decreased with the increase of H_2O_2 concentration. Therefore, this inhibition mode was speculated to be noncompetitive inhibition [43]. H_2O_2 as an inhibitor and Cu-Fe MOFs as enzymes could combine with the inactive sites to form H_2O_2-MOF complex, and then the complex combined with the substrate TMB. In other words, inhibitors had no effect on the binding of enzyme and substrate.

Under optimized conditions, the performance of this method was investigated in terms of linearity and limit of detection. The increasing amount of sodium sulfide was added to the colorimetric system. As shown in Fig. 2b, the corresponding UV–vis spectra were monitored and the absorbance peak at 652 nm gradually decreased and disappeared finally. With the increase of H_2S concentration, the absorbance difference tended to be stable (Fig. 2c). A strong linear relationship was observed between ΔA and H_2S concentration ranging from 0 to 80 μmol/L ($\Delta A = 0.0062c + 0.0088$, $R^2 = 0.997$), which was accompanied by a distinct color change from green blue to final light green (Fig. 2d). The limit of detection with naked-eyes and UV–vis spectrophotometer was 10 and 1.6 μmol/L, respectively, which were close to or lower than relevant MOF-based sensors, as shown in Table S2 (Supporting information). Our results also met the requirement of the World Health Organization for the detection of the maximum allowable level of H_2S in drinking water [11]. The obtained high sensitivity could be ascribed to the high affinity of Cu-Fe MOFs to the substrate and the subsequent occupation on the active sites of Cu-Fe MOFs by H_2S. Moreover, this method could be visual for end result with short assay time.

To evaluate the selectivity of bimetallic MOF sensor for detecting H_2S, several interfering substances (Cl^-, HCO_3^-, NO_3^-, NO_2^-, SO_4^{2-}, HPO_4^{2-}, $H_2PO_4^-$, Br^-, I^-, K^+, Al^{3+}, Ca^{2+}, Mg^{2+}, Zn^{2+}, Cr^{3+}, Cd^{2+}, Pb^{2+} and Mn^{2+}) that might exist in actual water samples were selected and added to the colorimetric sensing system respectively. The concentration of above solutions was 80 μmol/L, which was consistent with that of H_2S. As shown in Fig. 3, it was clear that upon addition of above substances, only H_2S could produce a significant decrease in absorbance at 652 nm, whereas the other interference caused no noticeable change of the absorption value after subtracting the baseline value. Our assay was specific for H_2S by direct visualization of the color change from green blue to final light green, while the solution color unchanged for the other interference. The high selectivity could be ascribed to the specific occupation on the active sites of Cu-Fe MOFs by H_2S. In contrast, other important components of wastewater were not absorbed on the surface of Cu-Fe MOFs. Thus, the outstanding advantages of this assay with characteristics of high sensitivity and selectivity could be applied in the detection of H_2S in real samples.

In order to verify the feasibility of the sensor in practical application, we applied it to the determination of H_2S in industrial wastewater and the samples were collected without pretreatment. No H_2S was found at detectable levels in the real samples and the same results were also confirmed by national standard method (GB/T 16489-1996). Hence, the recovery test was carried out by adding sodium sulfide standard solutions with different concentrations (40, 50 and 60 μmol/L), and the results were shown in Table S3 (Supporting information). The recoveries of H_2S in

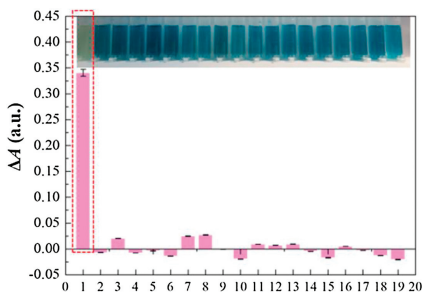

Fig. 3. UV–vis response and photographic image (inset) of the colorimetric assay upon the addition of 80 μmol/L substances including: (1) H_2S, (2) NO_3^-, (3) NO_2^-, (4) Al^{3+}, (5) I^-, (6) Mn^{2+}, (7) $H_2PO_4^-$, (8) HPO_4^{2-}, (9) SO_4^{2-}, (10) Cl^-, (11) K^+, (12) Br^-, (13) Ca^{2+}, (14) Mg^{2+}, (15) Zn^{2+}, (16) Pb^{2+}, (17) Cr^{3+}, (18) HCO_3^- and (19) Cd^{2+}, respectively.

wastewater samples ranged from 99.5% to 102%, and RSD ranged from 0.3% to 3.2%. The results show that the sensor had high accuracy and could be used for the rapid detection of H_2S in real samples.

In conclusion, we propose a colorimetric method for the detection of H_2S using the strategy of target-induced inactivation based on Cu-Fe MOFs as mimic enzymes. The results showed that the prepared MOFs had inherent peroxidase like activity and kinetic analysis showed that the catalyst was in accordance with the typical Michaelis-Menten kinetics. Compared with the reported MOF-based methods for detection of H_2S, the proposed sensor provides important advantages as follows: (i) Simplicity of the use of mixed-node Cu-Fe MOFs as the mimic enzymes without any modification, design, and complex synthesis; (ii) high sensitivity owing to the high affinity of Cu-Fe MOFs to the substrate; (iii) excellent selectivity due to the specific occupation on the active sites of Cu-Fe MOFs by H_2S; and (iv) easy and direct visualization of end result with color change. Our work will promote the application of MOFs in water quality analysis and environmental protection.

Declaration of competing interest

The authors report no declarations of interest.

Acknowledgments

The authors greatly appreciate the financial support from the National Natural Science Foundation of China (Nos. 21675109, 22074089), Central Thousand Talents Plan (No. ZYQR201810151), and Henan Joint International Research Laboratory of Chemo/Biosensing and Early Diagnosis of Major Diseases.

Appendix A. Supplementary data

Supplementary material related to this article can be found, in the online version, at doi:https://doi.org/10.1016/j.cclet.2021.02.053.

References

[1] H.C.J. Zhou, S. Kitagawa, Chem. Soc. Rev. 43 (2014) 5415–5418.
[2] I. Stassen, N. Burtch, A. Talin, et al., Chem. Soc. Rev. 46 (2017) 3185–3241.
[3] P. Kumar, A. Deep, K.H. Kim, TrAC Trend. Anal. Chem. 73 (2015) 39–53.
[4] X.Y. Ren, L.H. Lu, Chin. Chem. Lett. 26 (2015) 1439–1445.
[5] L.E. Kreno, K. Leong, O.K. Farha, et al., Chem. Rev. 112 (2012) 1105–1125.
[6] W.P. Lustig, S. Mukherjee, N.D. Rudd, et al., Chem. Soc. Rev. 46 (2017) 3242–3285.
[7] L.T. Liu, Y.L. Zhou, S. Liu, M.T. Xu, ChemElectroChem 5 (2018) 6–19.
[8] V.S. Lin, W. Chen, M. Xian, C.J. Chang, Chem. Soc. Rev. 44 (2015) 4596–4618.
[9] S.K. Pandey, K.H. Kim, K.T. Tang, TrAC Trend. Anal. Chem. 32 (2012) 87–99.
[10] Y. Luo, C.Z. Zhu, D. Du, Y.H. Lin, Anal. Chim. Acta 1061 (2019) 1–12.
[11] X.N. Liu, L.J. Huang, Y.P. Wang, et al., Sensor. Actuat. B: Chem. 306 (2020) 127565.
[12] Z.Q. Gao, D.Y. Tang, D.P. Tang, R. Niessner, D. Knopp, Anal. Chem. 87 (2015) 10153–10160.
[13] Z.H. Chen, C.Q. Chen, H.W. Huang, et al., Anal. Chem. 90 (2018) 6222–6228.
[14] Y. Liu, Y.L. Zheng, D. Ding, R. Guo, Langmuir 33 (2017) 13811–13820.
[15] C. Wang, G.Y. Ren, B.B. Yuan, et al., Anal. Chem. 92 (2020) 7822–7830.
[16] K. Vikrant, V. Kumar, Y.S. Ok, K.H. Kim, A. Deep, Tr A.C. Trend, Anal. Chem. 105 (2018) 263–281.
[17] Y. Ma, H. Su, X. Kuang, et al., Anal. Chem. 86 (2014) 11459–11463.
[18] X. Zhang, J.M. Zhang, Q. Hu, et al., Appl. Surf. Sci. 355 (2015) 814–819.
[19] X.Y. Wan, L.Q. Wu, L.C. Zhang, H.J. Song, Y. Lv, Sens. Actuators B: Chem. 220 (2015) 614–621.
[20] X. Zhang, Q. Hu, T.F. Xia, et al., ACS Appl. Mater. Interfaces 8 (2016) 32259–32265.
[21] A. Buragohain, S. Biswas, CrystEngComm 18 (2016) 4374–4381.
[22] X.F. Yang, H.B. Zhu, M. Liu, Inorg. Chim. Acta 466 (2017) 410–416.
[23] Y.P. Li, X. Zhang, L. Zhang, et al., J. Solid State Chem. 255 (2017) 97–101.
[24] Y.Y. Cao, X.F. Guo, H. Wang, Sensor. Actuat. B: Chem. 243 (2017) 8–13.
[25] X.B. Zheng, R.Q. Fan, Y. Song, et al., ACS Appl. Mater. Interfaces 10 (2018) 32698–32706.
[26] H.Z. Yu, C.Y. Liu, Y.H. Li, A.S. Huang, ACS Appl. Mater. Interfaces 11 (2019) 41972–41978.
[27] J. Zhang, F. Liu, J.L. Gan, et al., Sci. China Mater. 62 (2019) 1445–1453.
[28] Y.F. Shu, J.N. Hao, D.C. Niu, Y.S. Li, J. Mater. Chem. C 8 (2020) 8635–8642.
[29] W.M. Zhang, J. Wang, L.C. Su, et al., Sci. China Chem. 63 (2020) 1315–1322.
[30] X.L. Zhao, L.J. Zhang, J.G. Bai, et al., Spectrochim. Acta A 243 (2020) 118794.
[31] K. Tian, X.X. Wang, Z.Y. Yu, H.Y. Li, X. Guo, ACS Appl. Mater. Interfaces 9 (2017) 29669–29676.
[32] H.Y. Shang, H. Xu, L.J. Jin, et al., Sensor. Actuat. B: Chem. 301 (2019) 127060.
[33] J. Wang, Y.Y. Hu, Q. Zhou, et al., ACS Appl. Mater. Interfaces 11 (2019) 44466–44473.
[34] W.Y. Xie, M.L. Tian, X. Luo, et al., Sensor. Actuat. B: Chem. 302 (2020) 127180.
[35] H.X. Dai, W.J. Lü, X.W. Zuo, et al., Biosens. Bioelectron. 95 (2017) 131–137.
[36] Y.Q. Yin, C.L. Gao, Q. Xiao, et al., ACS Appl. Mater. Interfaces 8 (2016) 29052–29061.
[37] Y.L. Liu, X.J. Zhao, X.X. Yang, Y.F. Li, Analyst 138 (2013) 4526–4531.
[38] Y. Jiang, Q.-M. Yang, Q.J. Xu, et al., Anal. Biochem. 577 (2019) 82–88.
[39] R. Dalapati, S.N. Balaji, V. Trivedi, L. Khamari, S. Biswas, Sensor. Actuat. B: Chem. 245 (2017) 1039–1049.
[40] J.W. Zhang, M.C. Hu, S.N. Li, et al., Chem. Commun. 54 (2018) 2012–2015.
[41] J.J. Chen, H.J. Gao, Z.H. Li, Y.X. Li, Q. Yuan, Chin. Chem. Lett. 31 (2020) 1398–1401.
[42] C.J. Gao, H.M. Zhu, J. Chen, H.D. Qiu, Chin. Chem. Lett. 28 (2017) 1006–1012.
[43] Q. Fu, J. Tang, M. Cui, et al., J. Chromatogr. B 990 (2015) 169–173.